

Neotectonic and paleoseismicity studies on the Urumaco Fault, northern Falcón Basin, northwestern Venezuela

Franck A. Audemard^{a,*}, Jean-Claude Bousquet^b, José A. Rodríguez^{c,1}

^a *Funvisis, Apartado postal 76880, Caracas 1070-A, Venezuela*

^b *Laboratoire de Tectonophysique, Université Montpellier II, Montpellier, cedex 5, France*

^c *Litos C.A., Caracas, Venezuela*

Received 10 March 1998; accepted 2 December 1998

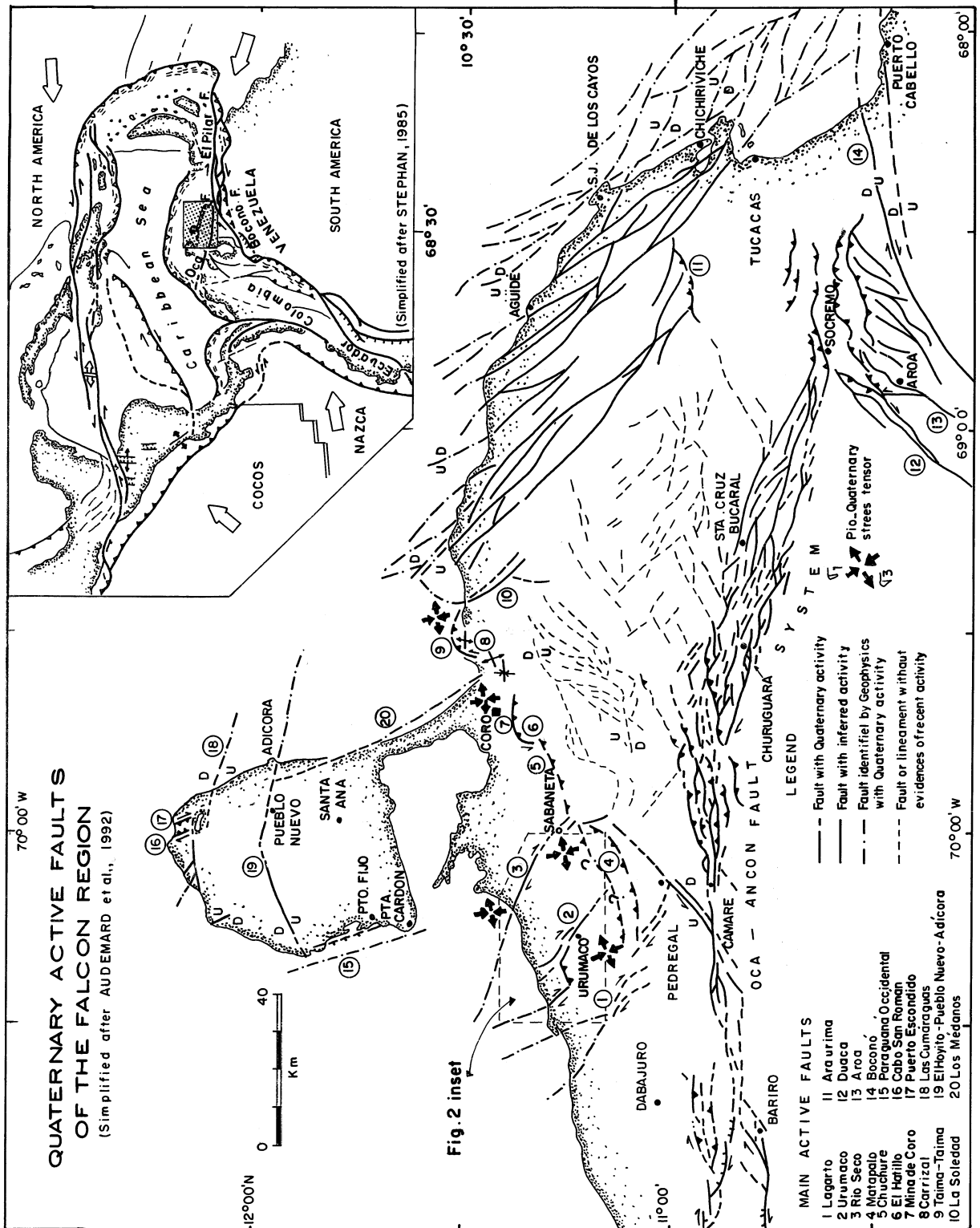
Abstract

The northern Falcón Basin in northwestern Venezuela is affected by several small active faults, subordinated to the major right-lateral east–west-trending Oca–Ancón Fault System. A set of prominent NW–SE right-lateral faults — synthetic shears — such as the Urumaco, Río Seco, Lagarto and La Soledad faults, stands out among those. The Urumaco Fault, located between the Lagarto and Mitare rivers (in the Urumaco Trough, west of Coro), presents a rather complex active fault trace that comprises two NW–SE fault segments linked by an ENE–WSW reverse echelon, all showing a restraining stepover geometry. Its western segment seems to continue to the north at sea. Conversely, the eastern one dies out on land and its northern tip ends in a transtensive horse-tail structure, that disrupts an Early Pleistocene conglomerate. This same unit is flexed and upheaved some 30 m at the restraining overlap. The kinematics and present stress tensor, the latest activity and the seismogenic potential of the eastern segment of the Urumaco Fault, have been assessed at a set of three river cuts of an ephemeral tributary stream of the Urumaco River, 3 km north of the Urumaco village, where the Urumaco Formation is truncated by a Late Pleistocene terrace (¹⁴C date of 20,700 ± 950 yr BP at the base) of the Urumaco River. On the one hand, one of these outcrops features the Urumaco Fault affecting the Late Miocene Urumaco Formation, which comprises two prominent fault planes disposed as a wedge. The southwestern bounding plane juxtaposes two different sequences whereas the northeastern one does not, implying different slip behavior. In fact, the northeastern plane shows oblique-slip striations (29°N, normal-dextral), whereas the other one shows perfectly horizontal striations (right-lateral). On the other hand, both updip plane prolongations in the overlying alluvial unit are not so sharp, if the 17-cm throw of the erosive bottom of such terrace measured at the lowermost part of the southwestern plane is regarded as an artifact. However, a mudflat deposit within this unit is bent with a 14-cm throw right above the northeastern fault plane clearly affecting the underlying Miocene unit. The estimated total offset per event allows to infer the occurrence of two individual events of magnitude ranging between M_s 5.8 and 6.4 on this strand of the eastern segment of the Urumaco Fault in the last 20,000 yr. © 1999 Elsevier Science B.V. All rights reserved.

Keywords: active tectonics; paleoseismology; seismic potential; Urumaco Fault; northwestern Venezuela

* Corresponding author. Fax: +58-2-257-9977; E-mail: faudem@funvisis.internet.ve

¹ Formerly at Funvisis.



1. Introduction

Northern Venezuela lies within the interaction zone between the Caribbean and South American plates (Fig. 1 inset). Although a general consensus exists about the eastward motion of the Caribbean with respect to South America (i.e., Hess and Maxwell, 1953; Bell, 1972; Malfait and Dinkelman, 1972; Jordan, 1975; Pindell and Dewey, 1982; Sykes et al., 1982; Wadge and Burke, 1983; Rosencrantz et al., 1988; Calais et al., 1989), this plate boundary is not of the simple right-lateral type. Instead, this is an over-100-km-wide active deformation zone, resulting from a long-lasting oblique-collision (Audemard, 1993a, 1995; Audemard and Giraldo, 1997). This implies that most of the southern Caribbean boundary has been mainly affected by transpression during the Tertiary, which is consistent with plate motion vectors proposed very early by Jordan (1975) and Minster and Jordan (1978), and later confirmed by recent GPS geodetic measurements (Freymueller et al., 1993; Lundgren and Russo, 1997).

The most conspicuous tectonic feature of the Falcón region in northwestern Venezuela is the east-west, right-lateral Oca–Ancón Fault System, that extends for about 650 km from the Colombian village of Santa Marta to the town of Boca de Aroa, located on the eastern coast of the Falcón State (Audemard, 1993a,b, 1994b, 1996c; Audemard et al., 1994). This fault system crosses the Goajira Peninsula, the outlet of Lake Maracaibo, the coastal plains of Buchivacoa (northwestern Falcón State) and the central Falcón Range (Fig. 1). It sharply truncates the northern terminations of the Santa Marta Block (northern Colombia) and Perijá Range (its summits constitute the Colombian–Venezuelan border). The Oca–Ancón System merges with the Boconó–San Sebastián–El Pilar System, considered by many workers as the major southern boundary of the Caribbean Plate (Hess and Maxwell, 1953; Rod, 1956; Molnar and Sykes, 1969; Minster and Jordan, 1978; Pérez and Aggarwal, 1981; Stephan, 1982; Aggarwal, 1983; Schubert, 1984; Soulas, 1986, 1989; Beltrán and Giraldo, 1989; among others), at the Aroa–Golfo Triste depression (Fig. 1).

Nevertheless, several secondary small active faults, subordinated to the Oca–Ancón Fault System, are also affecting the northern Falcón region (Audemard, 1993a, 1994a, 1997; Audemard and Singer, 1996). Among those, a set of prominent NW–SE right-lateral faults — synthetic Riedel shears — stands out southwest of Coro (in an area named as the Urumaco Trough by petroleum geologists), such as the Urumaco, Río Seco and Lagarto faults (Fig. 1).

The seismic hazard of the Falcón region has been basically assessed by a conventional neotectonic characterization. However, when possible, it has also been approached through paleoseismic studies, such as for (a) the Urumaco Fault, whose seismic potential is to be presented herein, and (b) the Oca–Ancón Fault System (Audemard, 1994b, 1996c). This seismic hazard assessment has not only focused on the contribution of each fault to the regional seismic hazard of a given site, but also on the associated ground deformations that these faults could generate.

2. Geological setting

The Tertiary Falcón Basin outcrops for some 36,000 km², comprising several states of northwestern Venezuela: the whole of Falcón and parts of Zulia, Lara and Yaracuy. Its sedimentary record is almost continuous since Late Eocene time, except for three angular and/or erosional unconformities of some regional extent, but not always widespread throughout the entire basin such as in the Urumaco Trough or in its eastern deep sea side (Audemard, 1993a). Thus, this region is exceptionally helpful for the understanding of the tectonic evolution of this part of the southern Caribbean Plate boundary.

The marine Oligo–Miocene Falcón Basin used to be the west end of the still active Bonaire Basin, which runs offshore along the Venezuelan Coast Range, until it was intensively folded and tectonically inverted by a NW–SE compression in Middle and Late Miocene times, then becoming an ENE–WSW elongated anticlinorium (Audemard, 1993a). Besides, sedimentation in this region since then has

Fig. 1. Quaternary active faults of the Falcón region in northwestern Venezuela (simplified after Audemard et al., 1992). Small inset at upper right corner shows relative location at plate tectonics scale. The relative location of Fig. 2 is also shown.

been restricted exclusively to the north flank of the Falcón Anticlinorium and sedimentary sequences have progressively become less marine and more continental. This inversion has been active until at least the Early Pleistocene based on the following facts (Audemard, 1993a): (1) the Pliocene La Vela Formation (shallow marine sequence) is in perfect upright position along the north limb of La Vela Anticline; (2) the Plio–Pleistocene Coro Formation, mainly composed of fan-conglomerates, dips 65°N; (3) the existence of two younger unconformities (Pliocene and Pleistocene in age). Moreover, this tectonic inversion must be still active as suggested by some local uplifted marine features (i.e., beachrocks, staircased marine terraces, etc.) along the northern coast of this region (Audemard, 1996a,b; Audemard et al., 1997).

3. Neotectonic setting

The recognition and latter evaluation of both brittle and ductile deformations affecting the Pliocene and Pleistocene formations that outcrop in the northern Falcón Basin, and particularly in the Urumaco Trough (southwest of Coro) where at various places several microtectonic stations were made, have allowed to establish that this region is undergoing a regionally consistent stress tensor characterized by a NNW–SSE to N–S maximum horizontal stress and an ENE–WSW minimum (or intermediate) horizontal stress (Audemard et al., 1992; Audemard, 1993a, 1997; Fig. 1). Reliable fault-plane kinematic indicators (steps, strololites, recrystallizations, Riedel shears, stylolitic peaks, tool marks) and/or gypsum fiber growth in some cases, were used to fix the sense of motion for each single fault plane. The timing of this ongoing compressional phase is certainly younger than the progressive tilting of the well-packed Late Pliocene–Early Pleistocene fan-glomerates of the Coro Formation, that is to say, Quaternary in age (Audemard, 1993a, 1997).

The present fault and fold spatial configuration at regional scale, local folding and minor genetically associated tectonic structures at fault terminations, such as horse-tail splays and pop-up at restraining stepovers, are in perfect agreement with kinematic indicators observed at microtectonic scale on fault

planes cutting Pliocene and Quaternary sedimentary units of the Falcón Basin. Therefore, the stress tensor calculated by means of the method by Etchecopar et al. (1981) well represents the stress field for the present-day kinematics of five sets of active faults (Fig. 1) in this region (Audemard, 1993a, 1994a, 1997; Audemard and Singer, 1996): (1) E–W right-lateral faults (Oca–Ancón Fault System, Adicora Fault); (2) NW–SE right-lateral faults, synthetic to the E–W faults (Urumaco, Río Seco, Lagarto and La Soledad faults); (3) NNW–SSE normal faults (western Paraguaná, Cabo San Román, Puerto Escondido and Los Médanos faults); (4) N–S to NNE–SSW left-lateral faults, antithetic to the E–W faults (Carrizal, El Hatillo and other minor faults); and (5) ENE–WSW reverse faults, parallel to folding axis (Araurima, Taima-taima, Chuchure and Mata-palo faults).

4. The Urumaco Fault

The Urumaco Fault roughly strikes NW–SE. Its right-lateral sense of motion has been established by geomorphic evidence (i.e., right-laterally offset drainages; Fig. 2), offset Neogene beds and several consistent-and-persistent microtectonic indicators on fault planes observed at three river cuts: two on an ephemeral creek that pours into the Urumaco River (black square on east edge of Fig. 2) and one on the Urumaco River itself, near the confluence of the Mamón Creek.

The Urumaco Fault has been mapped for over 30 km in length, affecting sedimentary rocks of the Urumaco Trough of Late Miocene age and younger, a sub-basin of the Tertiary Falcón Basin. In fact, its trace is not simple and presents two distinct 10-km-apart segments, linked by an ENE–WSW reverse fault (Fig. 2 inset), all disposed as a restraining stepover (Audemard, 1993a).

The eastern segment of the Urumaco Fault on land is the longest one, thus it is considered the main segment. It is composed of two, and occasionally three, subparallel strands and extends for 30 km from the Cuajarcume Bay to the Mosqueda Range, located east-southeast of the Urumaco village. Near the coast (Fig. 2), this main fault segment seems to become a transtensive horse-tail structure, since the early Qua-

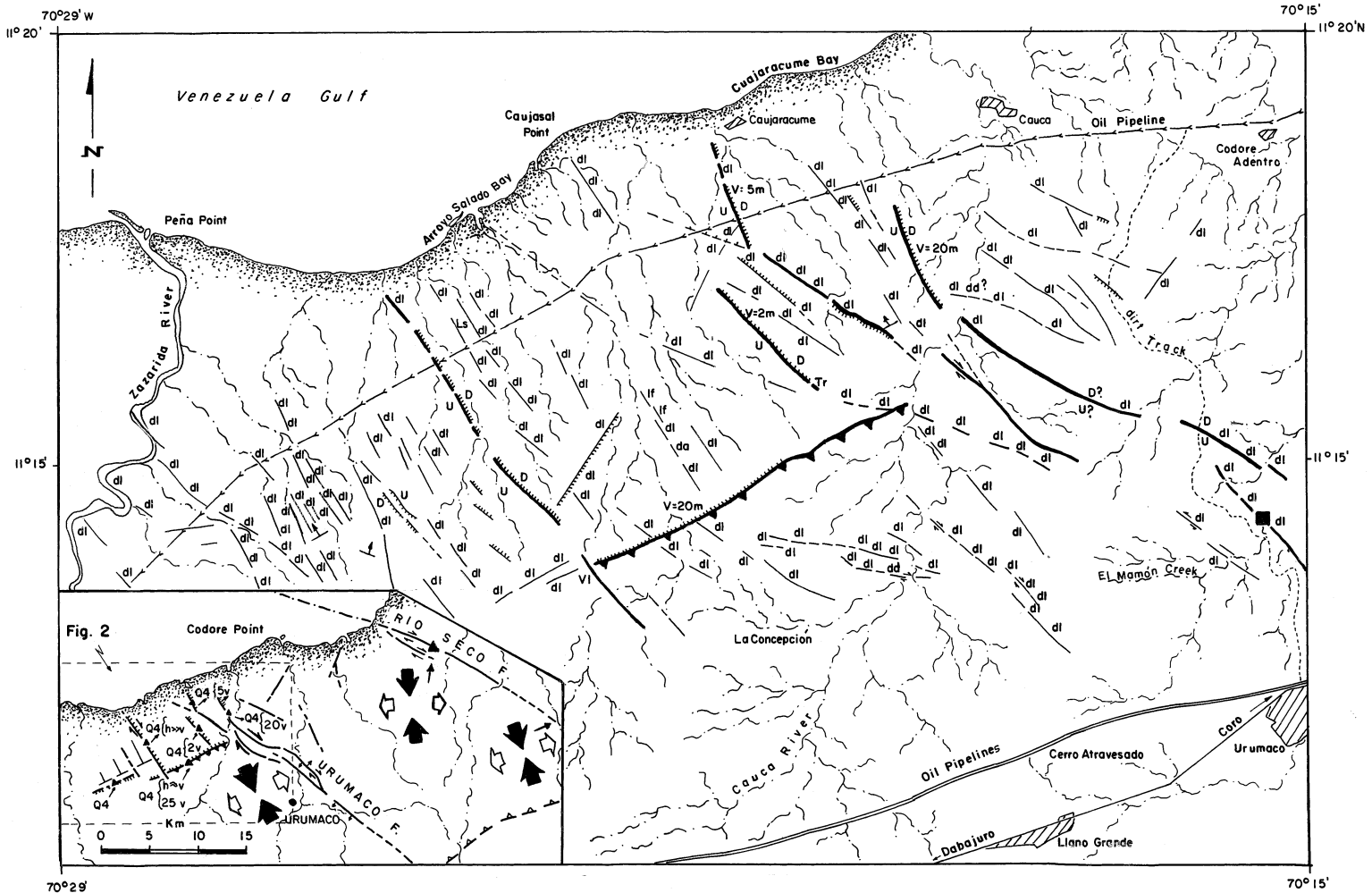


Fig. 2. Geomorphic evidence of Quaternary tectonic activity of the Urumaco Fault, between the Zazárida and Urumaco rivers, southwest of Coro (Audemard, 1993a). Small inset shows relative location of this figure, as well as Quaternary stress tensors calculated by Audemard (1993a, 1997) in the Urumaco Trough. Legend: *dd* = offset drainage; *dl* = linear drainage; *lf* = linear ridge; *ls* = line spring; *tr* = trench; *U/D*, up/down; $10 v = 10$ m of vertical throw; $h \approx v$ = similar horizontal and vertical offsets; Q_4 = Early Pleistocene, relative age of deformed geologic marker; bold lines indicate active fault traces; barbed lines represent fault scarps.

ternary (Q_4) cobble-sized alluvial pediments, which are truncating the Neogene sequence, are vertically offset between 2 and 20 m by a set of $N160^\circ$ -striking normal faults, whose scarps mainly face east (Fig. 2). The spatial disposition of these minor Quaternary normal faults confirm that (1) the post-early Quaternary slip of the Urumaco Fault is right-lateral, and (2) this eastern (main) segment does not continue farther northwest into the Venezuela Gulf shelf. Nearby Urumaco, this segment offsets Late Miocene and Pliocene beds less than 30 m right laterally. This evidence is not reliable for estimating a long-term slip rate, since this fault has had opposite senses of motion as suggested by the occurrence of apparent left-lateral offsets along subparallel minor faults to the Urumaco trend, like near the Mamón Creek, 3 km north of the Urumaco village (Fig. 2).

The second segment of the Urumaco Fault runs parallel to the main one, some 10 km west of it, closer to the Zazárida River (Fig. 2). This segment has only been mapped near the coast and shows a magnificent east-looking scarp affecting the same early Quaternary alluvial pediment as the main segment. This segment may continue offshore on the Venezuela Gulf shelf based on available seismic profiling of the shelf.

Both segments are kinematically connected by a reverse fault that strikes $N065^\circ$, whose surface expression is a flexural scarp preserved in the Q_4 alluvial pediment. This alluvial unit truncates most of this area between the Zazárida and Cauca rivers (Graf, 1969). This configuration, made of two subparallel segments linked by an orthogonal reverse fault, suggests an overall restraining stepover geometry, which is coherent with the right-lateral slip of the Urumaco Fault (Fig. 2). The Quaternary vertical throw of this reverse fault is estimated between 20 and 25 m, measured across the present flexural scarp topography.

5. Paleoseismic assessment of the Urumaco Fault

The three studied outcrops expose only one of the two-to-three strands of the main (eastern) segment of the Urumaco Fault that extends between the coast — Cuajarácume Bay — and the Mosqueda Range. These outcrops correspond to natural river cuts: one

belonging to the Urumaco River and the two others to a small ephemeral tributary, near the confluence of the Mamón Creek, located some 3 km north of the Urumaco village (black square on Fig. 2). The three outcrops are less than 250 m apart and only one was studied for paleoseismic purposes. No trenching was required during this study, although the conventional techniques in paleoseismic studies were applied.

5.1. Stratigraphy and structures

The three river cuts expose the Late Miocene Urumaco Formation (mainly a deltaic unit rich in reptile fossils: turtles and alligators) truncated by a rather flat-lying late Quaternary alluvial terrace of the Urumaco River. A ^{14}C dating of a charcoal fragment from the bottom of this alluvial unit has yielded an age of $20,700 \pm 950$ yr BP (sample VEN-UR01-90), thus confirming its late Quaternary age (Fig. 3).

The fault is clearly visible in the Late Miocene sequence (Urumaco Formation; Tm in Fig. 3) and can be followed from northwest to southeast through the three outcrops (Audemard, 1993a). The fault zone has a wedge shape where shearing is intense (Fig. 3). The wedge is bounded on the northeast by a normal-dextral fault ($N128^\circ 64^\circ S$; striations $29^\circ N$ of pitch) and on the SW by a pure dextral fault ($N120^\circ 70^\circ S$; horizontal striations). The northeastern bounding fault plane (Fault 1 on Fig. 3) does not seem to accumulate very much offset, whereas the right-lateral bounding fault plane (Fault 2 on Fig. 3) juxtaposes two completely different sequences of the same stratigraphic unit (Urumaco Formation). This suggests that Fault 2 is the main fault plane and Fault 1 bifurcates from it at the very near subsurface.

5.2. Description of recent deformation

On the northernmost of the three outcrops (Fig. 3), the late Quaternary alluvial deposits show very subtle deformation in association with both wedge-bounding fault planes. A clay layer within this alluvial unit (probably corresponding to a mud-flat deposit) is bent right above Fault 1 (Fig. 3). On the contrary, the very bottom of the same alluvial deposit is sharply cut by Fault 2, where a rather thin clay lens is clearly offset and two different alluvial

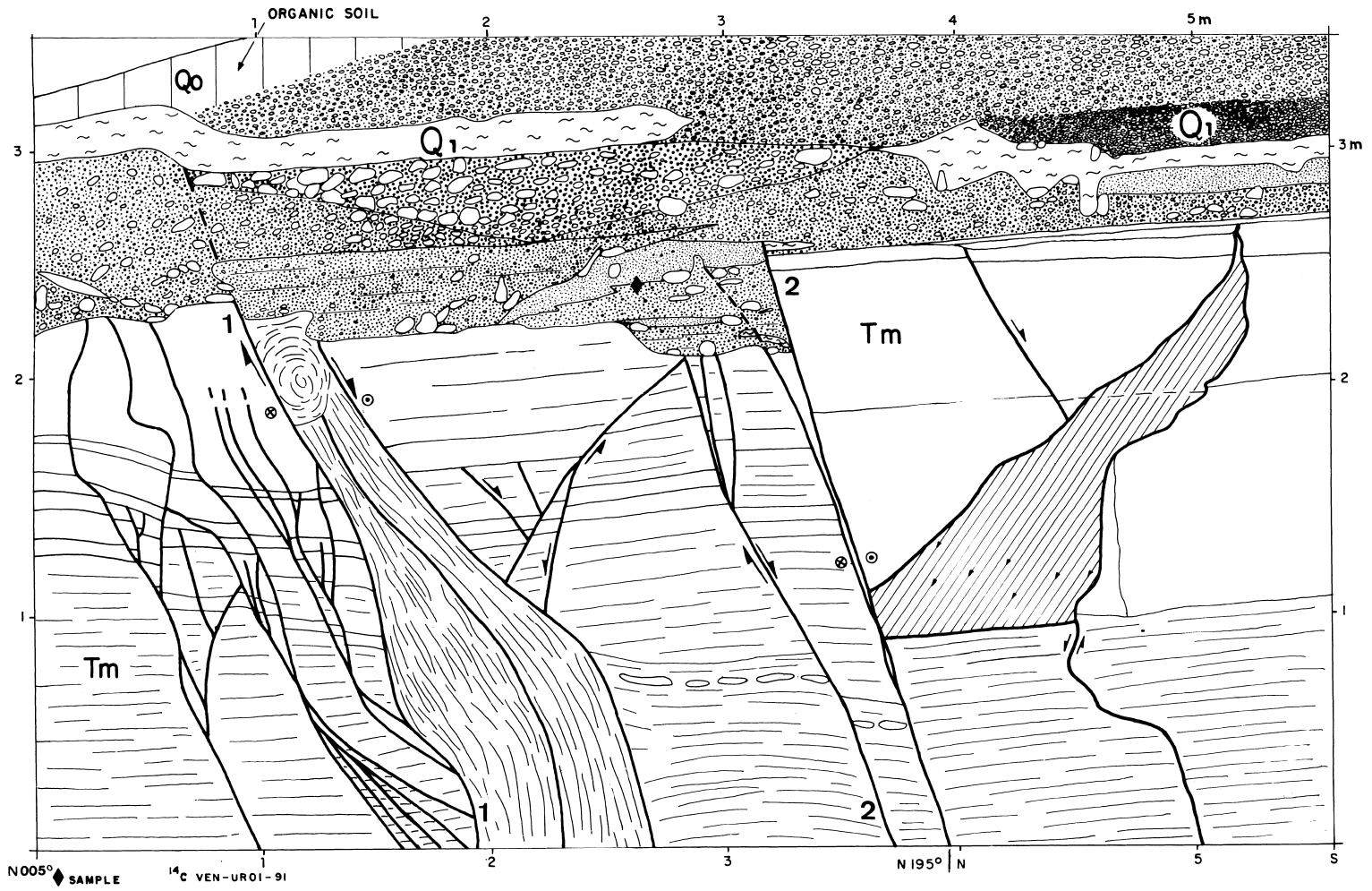


Fig. 3. Log of river cut near confluence of the Mamón Creek and Urumaco River, exposing an active strand of the eastern segment of the Urumaco Fault, that is composed of two wedge-bounding fault planes (after Audemard, 1993a). Location is indicated by a black square on the east edge of Fig. 2.

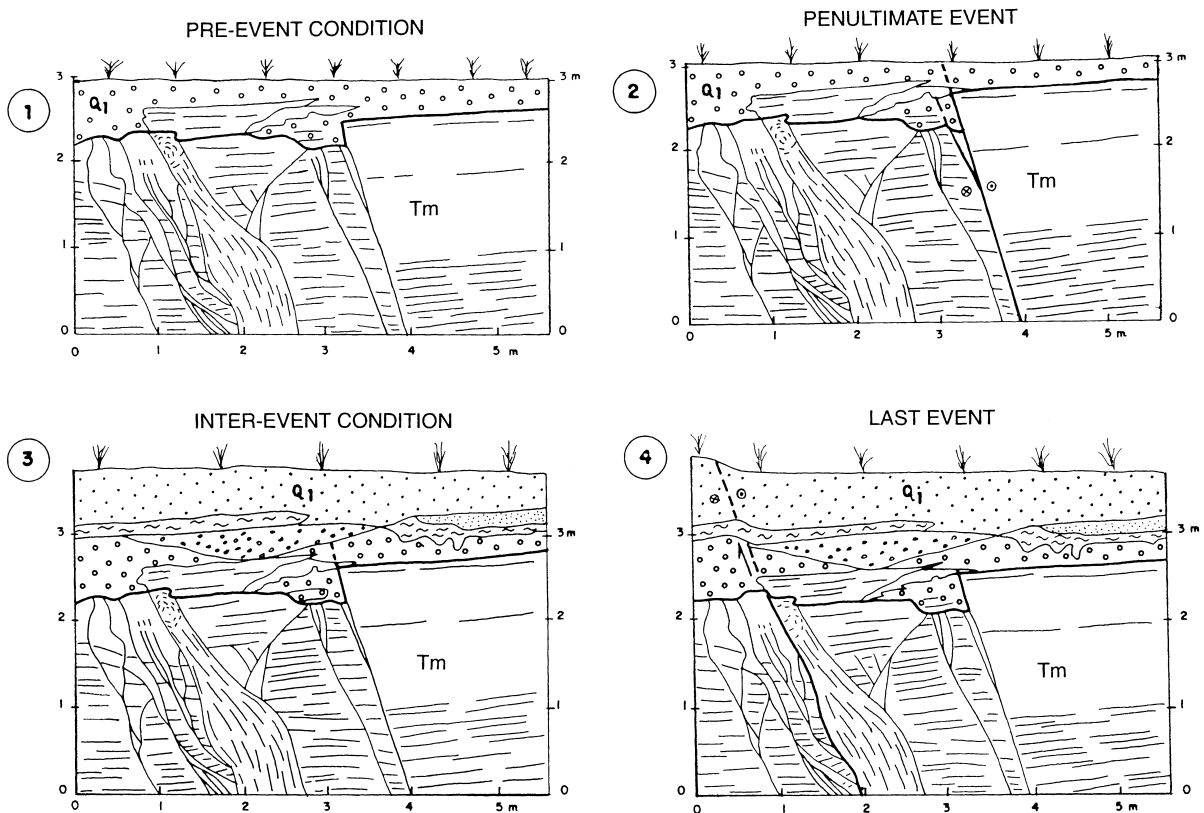


Fig. 4. Reconstruction of the last two events on one strand of the eastern segment of the Urumaco Fault (after Audemard, 1993a).

facies are juxtaposed; all been drowned by younger and coarser undeformed alluvial facies (Fig. 3). The vertical offset of the erosive bottom of the alluvial terrace on Fault 2 is an artifact, produced and magnified by differential erosion of the underlying Urumaco Formation because of intense fracturing concentrated in the fault-bounded wedge. This alluvial unit, as mentioned earlier, has been dated at about 20,000 yr BP, implying that this Urumaco Fault strand has been activated at least twice during such time span.

5.3. Paleoseismicity recognition

To decipher the number and size of paleoseismicity events that have occurred on this strand, a paleoseismicity reconstruction has been achieved (Fig. 4).

(1) A first event on Fault 2, to which an apparent vertical throw of 17 cm, measured on the erosional unconformity between the Quaternary and Late

Miocene sedimentary units, could be assigned (frame 2 of Fig. 4). However, this is an artifact as explained earlier. In fact, fault slip juxtaposes two different facies at the bottom of the late Quaternary alluvial terrace.

(2) A second younger earthquake on the other wedge-bounding fault (Fault 1), that bends the interbedded mudflat deposit within the late Quaternary alluvial unit of 14 cm vertically (frame 4 of Fig. 4). Fault 2 did not move at this time since the coarser alluvial deposit equivalent to the mudflat deposit is not disrupted above it.

These young — both brittle first and ductile later — deformations are sealed partially by a Holocene organic-poor soil, implying that this fault strand has moved in Late Pleistocene times and probably during the early Holocene as well.

Accordingly, these two wedge-bounding faults have moved independently and alternately: a first event on Fault 2 and a younger shock on Fault 1,

although it could have been expected that both faults would move simultaneously because they branch off from a single fault plane at very shallow depth.

5.4. Earthquake magnitude and slip rate

The penultimate event magnitude (frame 2 of Fig. 4) is hard to characterize since the vertical throw (17 cm) measured at the top of the Late Miocene unit is simply an artifact that results from the superposition of the following two processes. (a) Previous differential erosion of the underlying Urumaco Formation during alluvial terrace deposition. (b) The later right-lateral offset (east block moving southeast) of a gently north-dipping erosional unconformity between the overlying Late Pleistocene alluvial terrace and the underlying Miocene Urumaco Formation. However, the coseismic slip should be considered larger than the apparent vertical throw since striations on that fault plane are perfectly horizontal. Audemard (1993a), using the methodology described in Audemard and Singer (1996) — based on empirical relationships that correlate earthquake magnitude and coseismic slip with rupture area on fault plane — has estimated a magnitude M_s 6.4 for the eastern segment of the Urumaco Fault, based on a rupture length of some 22 km, to which corresponds a coseismic slip of some 60 cm. This figure seems compatible with a 17-cm apparent vertical throw observed on the studied river cut, although that throw cannot be used for earthquake magnitude estimates because it is not possible to know how much of the throw is actually due to erosion during deposition of the Quaternary alluvial terrace and prior to fault slip associated to the earthquake (Fig. 3).

On the other hand, the latest event is associated to a 14-cm vertical throw. This vertical offset corresponds to a total coseismic slip of 30 cm, taking into account that slip has to occur along striations of 29°N of pitch. Following the methodology of Audemard and Singer (1996), such coseismic slip could be related to earthquakes of magnitude M_s 5.8.

Timing of these two events cannot be better constrained since no sufficient datable materials were found, except for the only sample collected at the bottom of the Late Pleistocene alluvial unit, that dates the occurrence of both events within the last 20,000 yr. Moreover, only a maximum slip rate can

be calculated for this strand of the eastern segment of the Urumaco Fault. Considering that this strand has accumulated 90 cm of slip in the last $20,700 \pm 950$ yr, a maximized slip rate for this strand of 0.044 ± 0.002 mm/yr is estimated. Nevertheless, this value could only be part of the Urumaco Fault slip rate since it may comprise two slightly overlapped strands in the area of confluence of the Mamón Creek with the Urumaco River (Fig. 2).

Taking into account the overall restraining stepover geometry of the Urumaco Fault, another way of estimating its slip rate could be based on the Quaternary (post- Q_4) vertical throw of some 25 m of the flexural scarp. Assuming that such scarp is produced by a blind reverse fault plane dipping 30° in the last 1.5 m.y. (estimated age of the Q_4 alluvial pediment), a long-term shortening slip rate of the restraining stepover of about 0.033 mm/yr is calculated; a rate that needs to be shared between the two NW–SE parallel segments that are dying out at the stepover. Nevertheless, it may represent the overall slip rate of the Urumaco Fault. This second value is very similar to the previous one calculated from cumulative coseismic slip.

Soulas et al. (1987) have estimated the Urumaco Fault slip rate at 0.1 mm/yr based on a 2-km offset of the Lower Pliocene Codore beds. Besides, they think that this rate may be higher since the fault has moved in opposite directions during Pliocene and Quaternary times. However, in their offset estimate, they neglect two negative facts: (a) the possibility of occurrence of oblique slip on this fault, combined with (b) a gentle (10°–30°N) dip of the Neogene sequence that exaggerates the magnitude of apparent horizontal offsets. Therefore, a more reliable estimate of the slip rate for the Urumaco Fault is much less than 0.1 mm/yr and should be around 0.04 and 0.05 mm/yr. This would imply that the return period of earthquakes of magnitude M_s 6.4 on the eastern segment of the Urumaco Fault should be 12,000 to 15,000 yr, and half this recurrence if both segments of the fault happen to be similar in total length.

6. Discussion

The seismic hazard assessment of any given region in a complex active plate boundary zone, such

as northern Venezuela, needs to rely on a thorough neotectonic characterization of every single active tectonic feature. This should be complemented, when possible, with a paleoseismic evaluation of their seismic potential, because contemporary seismicity may not be easily ascribed to a particular active tectonic feature due to regional tectonic complexity, thus making inaccurate any seismological approach for linear seismic sources based only on Gutenberg–Richter law. Moreover, the technique of characterizing paleo-earthquakes by trenching has proved worldwide to be a powerful tool in areas where the instrumental and historical seismicity record are too short or incomplete basically because recurrence of moderate-to-large earthquakes is much longer than the written tradition of the region or country. This is mainly applicable to Africa, America and Australia, but also to some regions of Europe (i.e., France, Spain). The Urumaco Fault shows a seismic behavior that seems to fall into this type, since it is characterized by moderate earthquakes (events of magnitude ranging between M_s 5.8 and 6.4) with a very long return period (6000 to 7500 yr on any segment of the fault), as suggested by this study. On the other hand, when compared with the over-650-km-long dextral Oca–Ancón Fault System, the contribution of the Urumaco Fault to the seismic hazard of northwestern Venezuela is small, because its maximum credible earthquake is about one order of magnitude smaller than the one on the Oca–Ancón Fault System (M_s 6.6 against 7.5) and its return period is at least twice longer (Audemard and Singer, 1996). Despite all the facts mentioned above, on the one hand the occurrence of an event of magnitude ≥ 6 on the Urumaco Fault cannot be neglected, because of the associated risk for rather small neighboring settlements and their inhabitants (i.e., Urumaco, Llano Grande, Cauca, Codore Adentro, Sabaneta and Pedregal) and even larger towns located some 60 to 70 km away, such as Coro and Dabajuro (Figs. 1 and 2), when the type of housing is considered. Most dwellings in this area are made of ‘Bahareque’ (sugar cane-framed walls, plastered with a mud and grass mixture) with heavy tile roofs. The very recent (January 25, 1999) widespread housing collapse that occurred in the Colombian town of Armenia due to a shallow (35 km deep) moderate (m_b 5.9) local earthquake is an excellent proof

of this. On the other hand, in terms of national concern with regard to environmental impact and economic loss, permanent ground deformations associated to an $M_s \geq 6$ event could damage several oil pipelines of two of the major Venezuelan refineries, that are crossed by this secondary Riedel shear to the Oca–Ancón Fault System (Fig. 2). Both refineries are located at Punto Fijo (Judibana) and Punta Cardón (Fig. 1). In terms of ground deformations, the pipelines during their service life might undergo important concentration of stress at several places due to coseismic slip along the Urumaco Fault of several to about 60 cm (maximum horizontal slip estimated in this study), depending on which fault trace would slip. For instance, the northern pipeline could be subjected to the maximum estimated horizontal slip if the western segment behaves similarly to the eastern one (the segment paleoseismically assessed herein) and both segments of the Urumaco Fault are to generate earthquakes of the same magnitude (Fig. 2). On the contrary, the transtensive horse tail at the northern tip of the eastern segment could affect the northern pipeline in a distributed manner where several minor normal faults would show vertical throws of several centimeters (Fig. 2).

Let us point out that any active fault, regardless of its length and/or its seismic potential, should not be neglected in any seismic hazard assessment. For instance, loss related to the 1995 Hyogoken-Nanbu (Kobe) earthquake might have been minimized if the Nojima Fault had been better known, even though such fault is small with respect to the Pacific Subduction in terms of seismic potential. In that sense, a thorough neotectonic study is fundamental, even though the fault may not be paleoseismically assessed for countless reasons.

7. Conclusions

The Urumaco Fault is an active right-lateral strike-slip feature that cuts across sedimentary rocks of Late Miocene and younger age of the Urumaco Trough in the northern Falcón region, northwestern Venezuela. Its present sense of motion has been established from (1) geomorphic evidence of Quaternary activity, (2) kinematic indicators observed on fault plane (microtectonics) in Neogene and younger

rocks, and (3) folding and minor genetically associated tectonic structures at fault terminations affecting late Quaternary alluvial units, such as transtensive horse-tail splays and compressive features at restraining stepovers. It represents a synthetic Riedel shear to the major right-lateral, east–west-trending Oca–Ancón Fault System.

The active trace of the Urumaco Fault, which has been mapped for over 30 km in length on land, is not simple and comprises two distinct 10-km-apart segments, linked by an ENE–WSW reverse fault, showing an overall restraining stepover geometry. The eastern segment, the longest on land (about 22 km long), dips in a transtensive horse-tail splay to the north, suggesting that it does not continue offshore. The fault trace jumps 10 km sideward to a more western position. This western segment is only present by the coast and seems to prolong offshore to the north. The reverse fault is evidenced by a magnificent 25-m-high, north-facing flexural scarp.

Although a thorough neotectonic–paleoseismic evaluation has been performed on the Urumaco Fault, the seismic potential of this fault should be regarded in a probabilistic manner (maximum credible earthquakes of magnitude 6.4 should repeat every 6000 to 7500 yr on the entire fault) since it has not been possible to better constrain both the occurrence of past earthquakes (two events have been identified in the last 20,000 yr) and the forthcoming event, because the precise age of the last event is unknown and a rough return period has just been estimated (12,000 to 15,000 yr for M_s 6.4 earthquakes on the eastern segment of the fault). Besides, it has not been possible to conclude about either the eventual interaction between major and secondary active faults (in this case, between the Oca–Ancón Fault System and the Urumaco Fault) or the triggering effects induced by slip along a fault on the activation of a neighboring one. Nevertheless, the slip rate of this fault has been estimated at 0.04 to 0.05 mm/yr, based on a cumulative coseismic slip (about 90 cm accumulated during two unequal events) in the last 20,000 yr.

An important contribution of this paleoseismic assessment on the Urumaco Fault refers to the mobility of surface rupture along this secondary fault. If two consecutive events on a fault strand have occurred on two different fault planes (just a couple of meters apart) in the very shallow subsurface, as demon-

strated through this study, we should expect that the same process would happen among several strands of a fault, such as those composing the eastern segment of this fault, that are connected in depth. Only conclusive paleoseismic studies could verify this hypothesis but no suitable trenching sites had been located on the other strands and/or segments mainly because of aridity of the area and scarce distribution of Holocene deposits. Paleoseismic trenching would have also helped solving whether (a) the western segment moves independently, (b) motion on one segment promotes slip on the other one, or (c) the reverse fault at the restraining stepover would be the eventual locus of a much larger earthquake that would incorporate both contiguous segments.

From the seismic hazard viewpoint, the Urumaco Fault is not comparable to the Oca–Ancón Fault System since it may generate maximum credible earthquakes of one order of magnitude smaller, that would repeat twice less. However, a local $M_s \geq 6$ earthquake in a sparsely populated area where most dwellings are made of ‘Bahareque’ (low-resistant materials) with heavy tile roofs might be highly devastating. Moreover, a surface rupture along the Urumaco Fault with coseismic slip of some tens of centimeters (up to 0.60 m) might produce severe damage to oil facilities — mainly pipelines — that in turn might represent a significant negative impact on the Gross National Product. As a concluding remark, let us stress that no active fault, regardless of its length and/or its seismic potential, deserves to be neglected in any seismic hazard assessment.

Acknowledgements

This research was funded by Intevep, S.A. and Maraven, S.A. between 1990 and 1992, to which we are deeply indebted. We wish to thank our colleagues of the Earth Sciences Department of Funvisis, who helped during the field work, and the ILP II-3 and ILP II-5 colleagues: Daniela Pantosti and Spyros Pavlides, who encouraged this contribution. We are also grateful to the former Laboratoire de Géologie Structurale of the Université de Montpellier II where all the microtectonic analyses were carried out, and we particularly desire to acknowledge Drs. Alfredo Taboada Hoyos, Jean-François Ritz and Samira Re-

baï for their constant support and fruitful discussions. Part of this work would not have been possible without the wonderful drafting of Marina Peña (Funvisis) and Jojo Garcia (Montpellier II). This contribution was greatly improved by suggestions made by the reviewers Drs. Eutizio Vittori from ANPA, Italy, and Michel Sebrier from Université de Paris-sud, France.

References

- Aggarwal, Y., 1983. Neotectonics of the Southern Caribbean: recent data, new ideas (abstr.) *Acta Cient. Venez.* 34 (1), 17.
- Audemard, F.A., 1993a. Néotectonique, Sismotectonique et Aléa Sismique du Nord-ouest du Vénézuéla (système de failles d'Oca–Ancón). Ph.D. Thesis, Université Montpellier II, 369 pp.
- Audemard, F.A., 1993b. Trench investigation across the Oca–Ancón fault system, Northwestern Venezuela (extended abstr.). 2nd Int. Symp. Andean Geodynamics, Oxford, England, pp. 51–54.
- Audemard, F.A., 1994a. Neotectonics of the Falcon Basin, Northwestern Venezuela (abstr.). *Bull. INQUA Neotectonics Commission* 17, p. 74.
- Audemard, F.A., 1994b. Oca–Ancón Fault System: active trace and seismogenic characterization (northwestern Venezuela) (abstr.) *EOS* 75 (44), 611.
- Audemard, F.A., 1995. Geodynamic evolution of the Southern Caribbean: constraints from the geological history of the Falcón Basin, Venezuela. 14th Caribbean Geological Conf., Port of Spain, Trinidad and Tobago, pp. 11–12. Reprinted in *Bull. INQUA N.C.* 18, 49 (abstr.; paper in press).
- Audemard, F.A., 1996a. Field-trip guidebook to 'The late Quaternary marine deposits of the Paraguaná peninsula and Coro surroundings'. Ed. Funvisis, Caracas, 57 pp.
- Audemard, F.A., 1996b. Late Quaternary marine deposits of the Paraguaná peninsula, state of Falcon, northwestern Venezuela: preliminary geological observations and neotectonic implications. *Quat. Int.* 31, 5–11.
- Audemard, F.A., 1996c. Paleoseismicity studies on the Oca–Ancón fault system, northwestern Venezuela. *Tectonophysics* 259, 67–80.
- Audemard, F.A., 1997. Tectónica activa de la región septentrional de la cuenca invertida de Falcón, Venezuela occidental. 8th Congreso Geológico Venezolano, Porlamar, Venezuela 1, pp. 93–100.
- Audemard, F.A., Giraldo, C., 1997. Desplazamientos dextrales a lo largo de la frontera meridional de la placa Caribe, Venezuela septentrional. 8th Congr. Geológico Venezolano, Porlamar, Venezuela 1, pp. 101–108.
- Audemard, F.A., Singer, A., 1996. Active fault recognition in northwestern Venezuela and its seismogenic characterization: neotectonic and paleoseismic approach. *Geofís. Int. Méx.* 35 (3) (Suppl.), 245–255.
- Audemard, F.A., Singer, A., Beltrán, C., Rodríguez, J.A., Lugo, M., Chacín, C., Adrianza, A., Mendoza, J., Ramos, C., 1992. Actividad tectónica cuaternaria y características sismogénicas de los sistemas de fallas de Oca–Ancón (Tramo Oriental), de la Península de Paraguaná y región de Coro y de la costa nororiental de Falcón. Funvisis' unpubl. rep. for Intevep, 2 Vols.: 245 pp. (Vol. I), + 54 pp (Vol. II) + 4 appendices.
- Audemard, F.A., Singer, A., Rodríguez, J.A., Beltrán, C., 1994. Definición de la traza activa del sistema de fallas de Oca–Ancón, Noroccidente de Venezuela. VII Congr. Venezolano Geofísica, Caracas, Venezuela, pp. 43–51.
- Audemard, F.A., Rodríguez, J., Bousquet, J.-C., 1997. Evidence of Holocene tectonic uplift of the La Vela anticline related to the activity of the Guadalupe Thrust, northern Falcon State (Venezuela). In: Meco, J., Petit-Maire, N. (Eds.), *Proc. IV CLIP Meeting 1995*. Servicio de Publicaciones, Univ. de Las Palmas de Gran Canaria, pp. 13–27.
- Bell, J., 1972. Geotectonic evolution of the southern Caribbean area. *Geol. Soc. Am. Mem.* 132, 369–386.
- Beltrán, C., Giraldo, C., 1989. Aspectos neotectónicos de la región nororiental de Venezuela. VII Congr. Geológico Venezolano, Barquisimeto 3, pp. 1000–1021.
- Calais, E., Stephan, J.-F., Beck, C., Carfantan, J.-C., Tardy, M., Thery, J.-M., Olivet, J.-M., Bouysse, P., Mercier de Lepinay, B., Tournon, J., Vila, J.-M., Mauffret, A., Blanchet, R., Bourgois, J., Dercourt, J., 1989. Évolution paléogéographique et structurale du domaine caraïbe du Lias à l'Actuel: 14 étapes pour 3 grandes périodes. *C. R. Acad. Sci. Paris*, 309, 1437–1444.
- Etchecopar, A., Vasseur, G., Daignieres, M., 1981. An inverse problem in microtectonics for the determination of stress tensor from fault striation analysis. *J. Struct. Geol.* 3 (1), 51–65.
- Freymueller, J.T., Kellogg, J.N., Vega, V., 1993. Plate motions in the north Andean region. *J. Geophys. Res.* 98, 21853–21863.
- Graf, C., 1969. Estratigrafía cuaternaria del noroeste de Venezuela. *Bol. Inf. Asoc. Venez. Geol., Min. Pet.* 12 (11), 393–416.
- Hess, H., Maxwell, J., 1953. Caribbean Research Project. *Bull. Geol. Soc. Am.* 64 (1), 1–6.
- Jordan, T., 1975. The present-day motion of the Caribbean plate. *J. Geophys. Res.* 80 (32), 4433–4439.
- Lundgren, P., Russo, R., 1997. Crustal motions in the southern Caribbean and northern Andes region (pre-print). *J. Geophys. Res.*, 25 pp.
- Malfait, B., Dinkelman, M., 1972. Circum-Caribbean tectonic and igneous activity and the evolution of the Caribbean plate. *Bull. Geol. Soc. Am.* 83 (2), 251–272.
- Minster, J., Jordan, T., 1978. Present-day plate motions. *J. Geophys. Res.* 83, 5331–5354.
- Molnar, P., Sykes, L., 1969. Tectonics of the Caribbean and Middle America regions from focal mechanisms and seismicity. *Bull. Geol. Soc. Am.* 80, 1639–1684.
- Pérez, O., Aggarwal, Y., 1981. Present-day tectonics of south-eastern Caribbean and northeastern Venezuela. *J. Geophys. Res.* 86, 10791–10805.
- Pindell, J., Dewey, J., 1982. Permo-Triassic reconstruction

- of western Pangea and the evolution of the Gulf of Mexico/Caribbean region. *Tectonics* 1 (2), 179–211.
- Rod, E., 1956. Strike-slip faults of northern Venezuela. *Bull. Am. Assoc. Pet. Geol.* 40 (3), 457–476.
- Rosencrantz, E., Ross, M., Sclater, J., 1988. Age and spreading history of the Cayman Trough as determined from depth, heat flow, and magnetic anomalies. *J. Geophys. Res.* 93 (3), 2141–2157.
- Schubert, C., 1984. Basin formation along Boconó–Morón–El Pilar fault system, Venezuela. *J. Geophys. Res.* 89, 5711–5718.
- Soulas, J.-P., 1986. Neotectónica y tectónica activa en Venezuela y regiones vecinas. VI Congr. Geológico Venezolano, Caracas 10, pp. 6639–6656.
- Soulas, J.-P., 1989. Definition de l'actuelle limite sud de la Plaque Caraïbe (abstr.). *Eur. Geophys. Soc., 14th General Assembly Symp.* S1.2, Barcelona.
- Soulas, J.-P., Giraldo, C., Bonnot, D., Lugo, M., 1987. Actividad cuaternaria y características sismogénicas del sistema de fallas Oca–Ancón y de las fallas de Lagarto, Urumaco, Río Seco y Pedregal. Afinamiento de las características sismogénicas de las fallas de Mene Grande y Valera (Proyecto COLM). *Funvisis'* unpubl. rep. for Intevp. 69 pp. + appendices.
- Stephan, J.-F., 1982. Evolution géodynamique du domaine Caraïbe, Andes et chaîne Caraïbe sur la transversale de Barquisimeto (Vénézuéla). Thèse d'Etat, Univ. Paris, 512 pp.
- Sykes, L., McCann, W., Kafka, A., 1982. Motion of Caribbean Plate during last 7 million years and implications for earlier Cenozoic movements. *J. Geophys. Res.* 87 (B13), 10656–10676.
- Wadge, G., Burke, K., 1983. Neogene Caribbean plate rotation and associated central American tectonic evolution. *Tectonics* 2 (6), 633–643.